Digital Simulation for the Behavior of the Flow of Non-Newtonian Fluids in 90° Pipe Bend

Khalil Kahine, Ali Hammoud, Gilbert Accary

Abstract— There are many complex and important industrial fluids such as polymer solutions, suspensions, blood, paints, oils and greases exhibiting complex rheological behaviour. Several empirical rheological models have been proposed for representing the viscosity function of these non-Newtonian fluids. Among them, the Power law (Ostwald-de Waele) model is the most widely used and it was found to be very simple and versatile in describing shear-thinning (suspensions, emulsions, polymeric fluids) as well as shear-thickening (highly loaded suspensions of very fine particles; e.g., starch, plaster. . .) behaviour. In this paper, the non-Newtonian fluid flow in a 90° curved pipe is studied numerically to obtain the additional pressure loss coefficient resulting from the bend for different values of Reynolds.

Index Terms— CFD, 90° Pipeline, Non-Newtonian fluid, Pressure loss coefficient, Simulation.

Conflict of Interest:-K. Kahine, A. Hammoud and G. Accary state that there are no conflicts of interest.

I. INTRODUCTION

Fluids are a major part in any industry. The usage of any fluid in industry requires its transport in pipelines, these pipe lines contains many singularities from diffusers, elbows, pumps and others. So for a good design of these pipelines one must have a good overview of the laws governing this flow and the losses in pressure from this law and how does the fluid behave in these pipes to have a control over them.

The fluids with nonlinear behaviour [5] conforms to the known power law; they are nevertheless considerably less studied compared to Newtonian fluids. The consequences of shear thinning need to be identified for a better understanding of the structure of the flow.

The assumption that the flow is fully developed in regions where it remains under strong influence of the inlet boundary conditions can seriously underestimate the design of flow systems and incorrectly assume specific velocity profile shapes leading to wrong conclusions in the interpretation of data [11].

A detailed discussion of the inconsistencies and confusion in literature is provided by Durst et al. [10], who conducted a detailed numerical study and proposed nonlinear correlations for pipes and channel for Newtonian fluids.

Khalil Kahine, Doctoral School of Science and Technology, Lebanese University, Beirut, Lebanon

Ali Hammoud, Doctoral School of Science and Technology, Lebanese University, Beirut, Lebanon

Gilbert Accary, Doctoral School of Science and Technology, Lebanese University, Beirut, Lebanon

In this paper, one is interested in the laminar flow of the non-Newtonian shear thinning fluids, in a 90 degree pipe bend (Fig.1).

The mathematical model is represented by the equations of continuity and conservation of movement quantity [8]. The Rheological behaviour is given by the power law of (Ostwald of Waele). We intend to determine by numeric way the structures of the dynamic fields of this flow. In addition, we are going to study the influence of Reynolds number and the shear thinning characters on the dynamic field and on the evolution of the pressure loss and the establishment length.

The development or the use of software is indispensable to the resolution of this kind of problems. The discretization of the system of equations is done numerically by finite volume method that is implemented to numerical modelling software "Ansys-Fluent" [8].

In pressure drop calculations it is an accepted practice to consider that the flow is fully developed in straight pipes, while all other effects (flow distortions, redevelopment) in a sudden symmetric expansions/contractions, pipe bends and other obstacles are introduced using local loss coefficients.

II. MATHEMATICAL MODEL

The general equations governing the laminar flow of incompressible fluids are:

(i). Continuity Equation

$$div\left(\rho \vec{V}\right) = 0 \tag{1}$$

(ii). Movement Equation

$$\rho \frac{d\vec{v}}{dt} = -\overrightarrow{grad}(p) + div(\vec{\tau}) \tag{2}$$

$Where$ $\vec{V}$ is the velocity vector, $\vec{\tau}$ the stress tensor, ρ the density and p the pressure.

The general conservation equations governing the isothermal flow in pipes are written by adopting the system of cylindrical coordinates.

In addition the following simplifications are adopted:

1. Stationary flow.
2. Incompressible flow (density is constant).
3. Axisymmetric flow in cylindrical pipe.
4. The radial pressure gradient is negligible.

(iii). Simplified Continuity Equation

$$\frac{\partial(ru)}{\partial z} + \frac{\partial(rv)}{\partial z} = 0 \qquad (3)$$

(iii). Simplified Movement Equation in z Direction

$$\rho u \frac{\partial u}{\partial z} + \rho v \frac{\partial u}{\partial r} = -\frac{dp}{dz} + \frac{1}{r}\frac{\partial}{\partial r}\left(r\mu_a \frac{\partial u}{\partial r}\right) + \frac{\partial}{\partial z}\left(\mu_a \frac{\partial u}{\partial z}\right) \qquad (4)$$

(iv). Simplified Movement Equation in r Direction

$$\rho u \frac{\partial v}{\partial z} + \rho v \frac{\partial v}{\partial r} = \frac{\partial}{\partial r}\left(\frac{\mu_a}{r}\frac{\partial(rv)}{\partial r}\right) + \frac{\partial}{\partial z}\left(\mu_a \frac{\partial v}{\partial z}\right) \qquad (5)$$

In addition to the following boundary conditions:

(v). Condition of non-sliding at the wall

$$u(r = R) = v(r = R) = 0 \qquad (6)$$

(vi). At the axis of symmetry

$$\frac{\partial u}{\partial r}(r = 0) = \frac{\partial v}{\partial r}(r = 0) = 0 \qquad (7)$$

For the problem of the establishment length, we have a constant axial velocity profile:

$$\frac{u}{u_m}(z = 0) = cte = 1 \qquad (8)$$

Where r is the pipe radius, u the axial velocity, v the radial velocity, μ_a is the apparent viscosity and u_m is the mean velocity.

The Simulation was done by the software "fluent" using the model of Herschel-Bulkley [5] for $\tau < \tau_0$.

We note that the equation used is Ostwald de Waele, but to solve this problem having our study fluid of this type, we choose to adopt as law behavior the equation corresponding to Herschel-Bulkley fluids in non-Newtonian critical stress. Recall that the model of Herschel-Bulkley is given by:

$$\tau = \frac{\tau_0 + K\left[\gamma^n - \left(\frac{\tau_n}{\gamma}\right)^n\right]}{\gamma} \qquad (9)$$

Having τ_0 "the yield stress threshold" equal to zero the preceding equation becomes the Ostwald de Waele equation:

$$\tau = K \times |\dot{\gamma}|^{n-1} \times \dot{\gamma} \qquad (10)$$

The consistency K of the fluid is found in terms of Reynolds number Re and the power index n for a cylindrical pipe and in between two plates [4]:

$$Re_n = 8^{1-n}\left(\frac{4n}{3n+1}\right)^n \frac{\rho u_m^{2-n} D^n}{K} \qquad (11)$$

$$Re_n = 12^{1-n}\left(\frac{3n}{2n+1}\right)^n \frac{\rho u_m^{2-n}(2e)^n}{K} \qquad (12)$$

In this chapter, we have established the mathematical partial differential equations governing the laminar flow of non-Newtonian pseudoplastic fluid and the software used "Ansys-Fluent" is responsible for the discretization and numerical solution.

III. NUMERICAL MODELLING

(i). Geometry and Boundary Conditions

The geometry of a pipe bend is shown schematically in (Fig.2) together with the coordinate system adopted. It is composed of a 90° bend of curvature radius, upstream and downstream tangents of length L1 and L2. For solving the governing equations, at the inlet, an axial velocity is assigned a fully-developed laminar velocity profile. The fully developed velocity profile for the inlet conditions was prepared for each Reynolds number. To obtain significant results, simulating as much as possible the actual fluid flow, passes first through a good discretization of the flow field. Recall that the golden rule of a good mesh is more finely meshed possible areas subject to strong variations of flow parameters and especially the entrance area of the pipe, where the maximum disturbance is due to the singularity of start-up. In our case, the mesh is made in "Ansys", this software allows the design of the geometry of the flow, the discretization of its edges, the mesh flow areas and to define the type of each side (boundary conditions) as shown in figure 1. It was agreed to appoint a mesh with a pair of numbers corresponding respectively the numbers of discretization points of the sides of the flow field, respectively in the axial and radial direction.
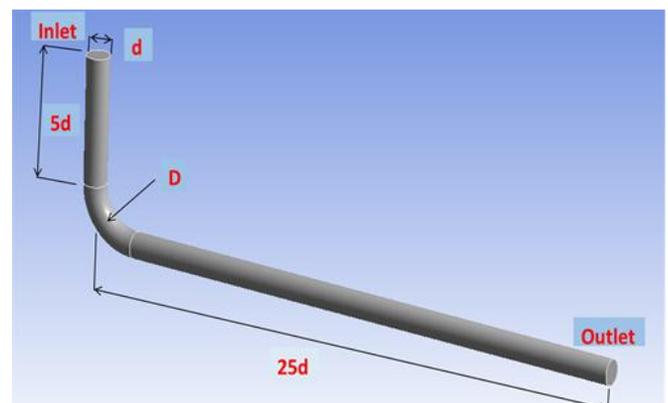
Figure 1: The geometry of the 90° bend pipe under consideration with boundary conditions. d and D are respectively the pipe and the bend curvature diameters.
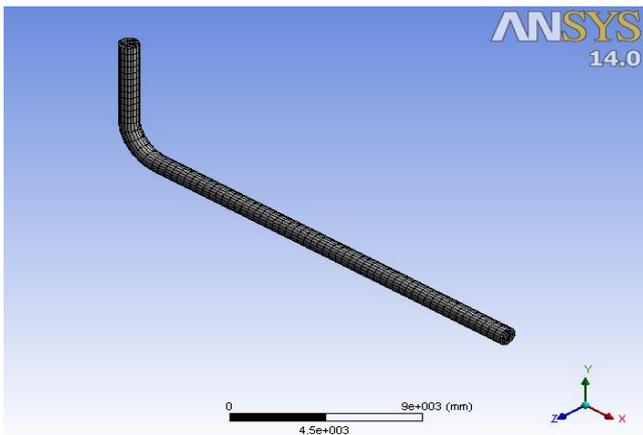
Figure 2: The 3-dimensional mesh draw using "Ansys".

(ii). Numerical Procedure and Simulation

The components of speed in the equations of momentum are bound to the pressure, which creates a main difficulty for their mathematical resolution. Indeed, if the field of pressure is taken in account in the treatment of these equations, the gotten speeds verify the equation of continuity, but the pressure is a fully-fledged variable, although it doesn't have an equation. We use a method of speed prediction-correction then according to the pressure; the equation of conservation of the mass is transformed to get pressure equation, so that the solution of the streamlined problem gives a field of speed and pressure verifying the equations of momentum and continuity equation.

We introduce the flow parameters in the software where the law of (Ostwald de waele) is defined rheological for the non-Newtonian fluid of index n and consistency K; where K is obtained from Reynolds and n using the equation (11) for cylindrical coordinate system.

The transport equations are solved by a fully-implicit finite volume method in a segregated formulation on an unstructured staggered mesh. Space discretization is based on the power law scheme for the convection terms while diffusion terms are approached by central difference approximation and the velocity pressure coupling is treated using SIMPLER algorithm [9]. A steady-state solution is supposed to be obtained when the residuals of all transport equations reach in non-dimensional form.
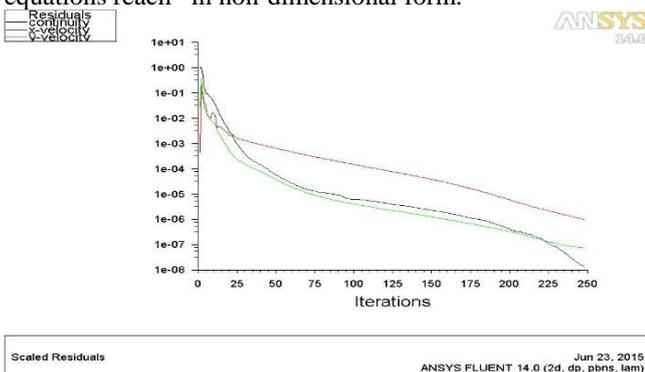
Figure 3: Evolution of simulation residual values.

The residual effect shows that for every point we have a number of iterations take place in order to converge to the solution the process repeats itself continuously to have a convergence limit. The final convergence is determined by measuring residual source of each variable. The residual sources are defined for each variable at each point and for each iteration.

As we can see from the above graph(fig 3) that values and coincide on each other, the value of was enough as convergence criterion. It starts the simulation and it makes the number of iterations needed to reach convergence.

(ii). Velocity Profile

In the entrance zone before the pipe bend we have an established velocity profile which is in an increasing way until it takes the parabolic form as shown in the following figure 4. The velocity profile in the entrance zone is expressed in equation (12):

$$\frac{u(r)}{u_m} = \left(\frac{3n+1}{n+1}\right)\left[1 - \left(\frac{r}{R}\right)^{\frac{n-1}{n}}\right] \qquad (12)$$

Where r is the radial distance of the flow, the radius of the pipe R=0.5 and $0 < r < R$. "u" is calculated and the obtained results for n= 0.3, 0.4, 0.6, 0.8 and 1are listed in the following graph (5):
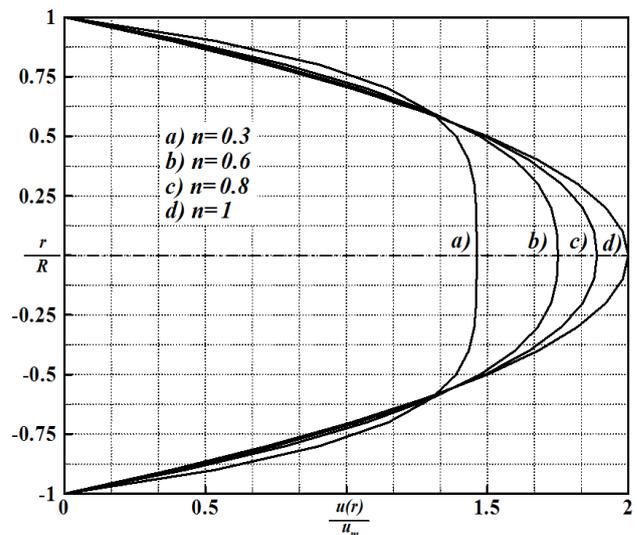
Figure 4: Inlet Velocity profile [3]

We observe in fig. 4 that as "n" decreases the plasticity zone increases and the shear rate deformation occurs more on the edges of the surface, and when the index structures reaches 1 which corresponds to Newtonian behavior ;the fluid is not affected by shear deformation and it moves smoothly.

Once the mesh is achieved; we can start the numerical calculation. The simulations are performed on "Ansys-fluent". This software has a user interface that allows easy handling, a significant display and easy access to Digital results, which makes software responsible to run a simulation.

We introduce flow parameters software and especially the law is defined theologically for the fluid used by the index

structure 'n' and by the consistency K as shown in the following figure 5.
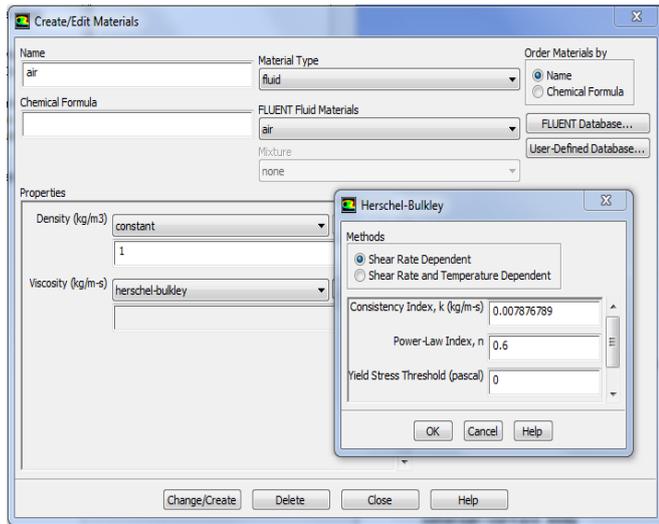
Figure 5: Input parameters

IV. PRESSURE DROP AND CORRELATION

(i). Pressure Evolutions

Numerical results are obtained for different values of Reynolds number ranging from 50 up to 1000, for a structure index varying between 0.3 and 1, and for different values of the geometric ratio D/d. we plot the pressure as a function of the center line of pipe bend.

We plot simultaneously for every Reynolds number the corresponding power law indexes n ranges between 0.3 and 1. For example figure 6 shows the evolution of the pressure (made dimensionless using the square root of the flow mean velocity) at the centerline of the pipe for Re = 250, D/d = 6 and for different values of n. Figure 7 shows the evolution of the pressure drop coefficient as a function of the Reynolds number for D/d = 4 and for different values of n.
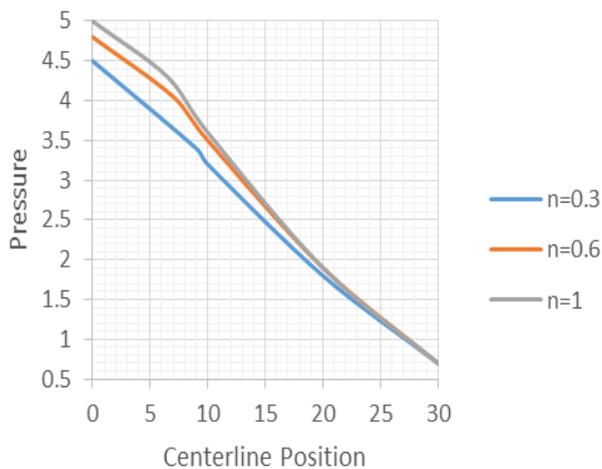
Figure 6: Evolution of the pressure at the centerline of the pipe for Re = 250, D/d = 6 and for different values of n.
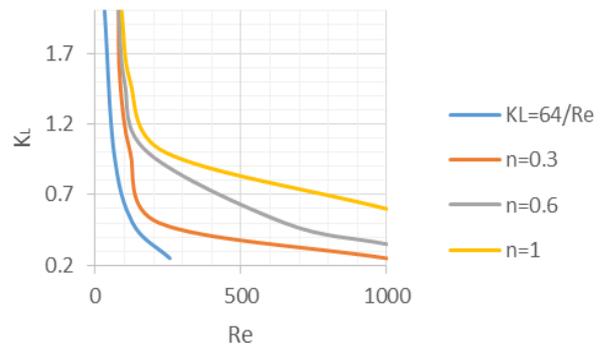
Figure 7: Evolution of the pressure drop coefficient as a function of the Reynolds number for D/d = 4 and for different values of n

The above figures (6-7) are two of many graphs that we have achieved by making different simulations varying (D/d, Re, n). In the next section we are interested to get a correlation for the pressure drop coefficient covering the range of the control parameters (Re, n, and D/d).

(ii). Correlation and results

In this study, correlations for the pressure drop coefficient were obtained covering the range of the control parameters (Re, n, and D/d) due to the presence of the elbow in the cylindrical pipe applying the following equation:

$$\frac{L_{equiv}}{L_{elbow}} = \frac{K_L}{32/R_e} \times \frac{4}{\pi(D/d)} \qquad (13)$$

Where K_L is the pressure drop coefficient in the pipe, L_{equiv} is the equivalent length of the pipe assuming it is straight and L_{elbow} is the length of the pipe bend.

Knowing K_L we can set up $\frac{L_{equiv}}{L_{elbow}} - 1$ as a function of Reynolds and trace it in the following graph.

For example figure (8) represent the evolution $\frac{L_{equiv}}{L_{elbow}}$ for D/d =2 as a function of Reynolds for different values of n ranged from n=0.3 to 1.
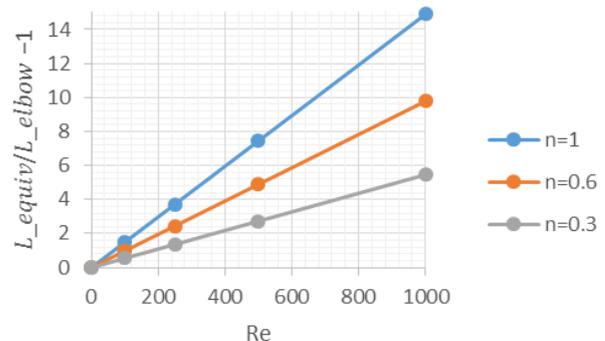
Figure 8: Evolution of L_eq/L_elbow as a function of Reynolds number for different values of n for D/d=2

As we can see from the above graph that each line passes through the origin which insure the fact that as Re tend to zero $\frac{L_{eq}}{L_{elbow}}$ tends to 1 and as D/d tends to infinity $\frac{L_{eq}}{L_{elbow}} = 1$

After doing similar graphs for D/d=3, 4, 5, 6 and 8. The function $\frac{L_{eq}}{L_{elbow}} = f(Re_n)$ is found to be similar to the relation:

$$y = A(n) \times Re \tag{14}$$

Where A (n) is the slop of the curve above.

In order to find the correct correlation between (n, Re and D/d) we draw the evolution of the slope A (n) as a function of n=0.3, 0.4, 0.6, 0.8 and 1 for different values of D/d as shown in figure 9.
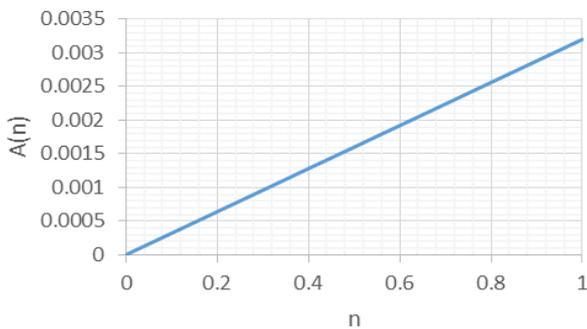
Figure 9: Evolution of the slopes for different index structure (n) for D/d=6.

The other graphs are similar to this one but instead of showing them we show their respective equation in the following table.

D/d	A(n)
D/d=2	$1.560E^{-02}$ n
D/d=3	$8.104E^{-03}$ n
D/d=4	$5.228E^{-03}$ n
D/d=5	$3.894E^{-03}$ n
D/d=6	$3.201E^{-03}$ n
D/d=8	$2.375E^{-03}$ n

Table 1: Slope A (n) as a function of D/d and n

Now, the same procedure we are interested in the evolution of the slope A (n) as a function of D/d.

The evolution is presented in fig.10.
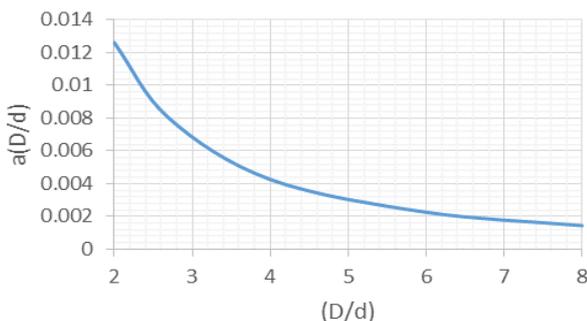
Figure 10: Evolution of the slopes as a function of (D/d).

We have

$$A(n) = a\left(\frac{D}{d}\right) \times n \tag{15}$$

And

$$a\left(\frac{D}{d}\right) = 3.74E^{-02}(D/d)^{-1.368} \tag{16}$$

Then,

$$A(n) = 3.74E^{-02}(D/d)^{-1.368} \times n \tag{17}$$

Finally we have:

$$\frac{L_{eq}}{L_{elbow}} = \{3.74E^{-02}(D/d)^{-1.368} \times n\} Re + 1 \tag{18}$$

So the pressure drop coefficient correlation:

$$K_L = \frac{32}{Re} \times \frac{L_{equiv}}{n} \tag{19}$$

$$K_L = 8\pi\left[\{3.74E^{-02}(D/d)^{-1.368} \times n\} + \frac{1}{Re}\right] \tag{20}$$

V. DYNAMIC STUDY OF THE ESTABLISHMENT LENGTH

In this chapter we will study the behaviour in the pipe elbow area, a non-Newtonian fluid non-complex thermo-dependent flowing in a cylindrical industrial pipe, where the axial velocity profile constantly evolving until it takes its final shape of establishment for laminar flow.

The establishment length can be calculated using the formula below figure 11:

$$L_{etab.} = 50 + U_{97\%} - Ltot \tag{21}$$
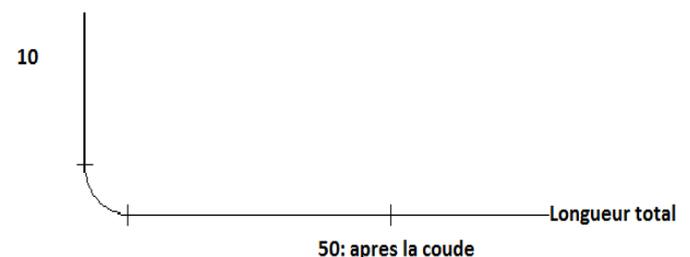
Figure 11: Establishment length

The axial velocity was found from our numerical study for several Reynolds numbers and power indexes as the example below figure 12:
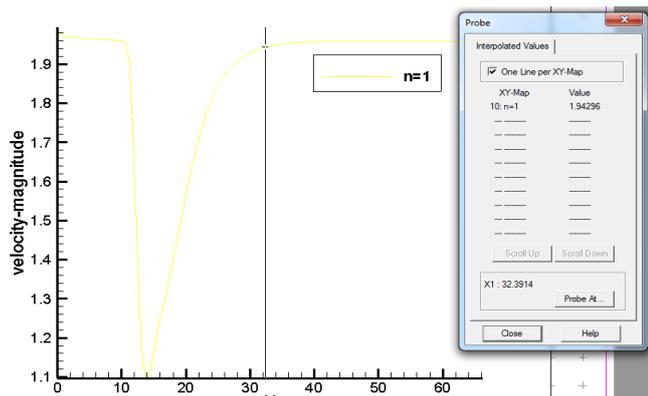
Figure 12: Axial velocity

Some study results are grouped in the tables below:

n\RE	50	100	250	500	1000
0.3	___	1.4676	8.7651	18.1928	34.7112
0.4	___	2.3012	10.1774	20.1083	39.3219
0.6	1.3705	3.9501	11.9056	23.961	50
0.8	1.968	4.9708	13.5459	28.6624	54.429
1	2.4188	5.6697	15.3815	31.102	58.429

Table 2: Establishment length for D/d=2 for deferent Re and n values

Following the same steps as in the pressure drop study we can reach for a correlated form for the establishment length.
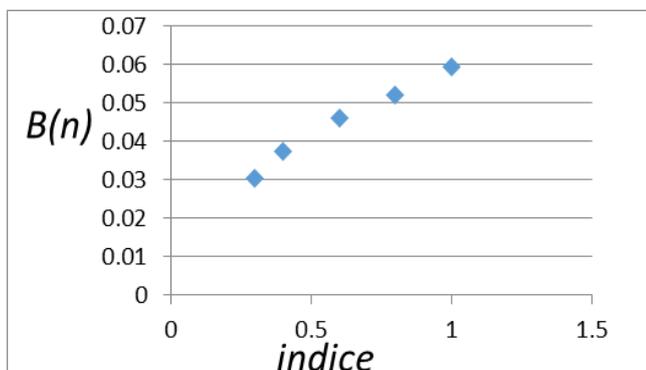
Figure 13: Variation of the slope B(n) as a function of index n for D/d=2

The establishment length can be correlated in the form of:

$$L_{etab.} = B(n).Re \qquad (22)$$

Where B(n) is of the form:

$$B(n) = bn^a \qquad (23)$$

The final form for the establishment length was found to be:

$$L_{etab.} = \left[-0.001 \left(D/d \right) + 0.062 \right] n^{[0.084(D/d) + 0.226]} \times Re \qquad (24)$$

VI. CONCLUSION

Steady and laminar flow of a non-Newtonian fluid in a 90° pipe bend was studied numerically taking the advantage of Ansys and fluent programs numerical codes.

First a theoretical approach was used in order to obtain the equation for pressure loss that occurs due to a presence of a pipe bend. To do so, one-dimensional analysis for the fully developed pressure drop in a straight pipe was incorporated in the overall pressure drop that occurs in a pipe bend as well as in an upstream and downstream tangent.

Meshes, was performed to study the influence of grid refinement on numerical predictions. In addition, a technique was used to quantify the numerical results for the total pressure drop (ptot) and the pressure drop between the entrance and exit of a bend (pbend).

After we found the pressure drop coefficient we had made a correlation to find the equivalent pipe bend length.

This study needs continuity and requires the study of the influence of various peculiarities already mentioned on dynamic and kinetic aspects using the software calculations adopted.

REFERENCES

[1] A. B. METZNER, Heat Transfer in Non-Newtonian fluids.
[2] N.MIDOUX, Mécanique et Rhéologie des fluides en génie chimique (1985).
[3] D. C. H. CHENG, A design procedure for pipeline flow of non-newtonian dispersed systems.Proc. Hydrotransport 1, 1st-10th September 1970, Page J5-77 à J5-95.
[4] K. Kahine, Simulation Numérique de l'Ecoulement de Fluides non-Newtoniens Lors du Franchissement d'un divergent. Lois de transfert de chaleur en conduite
[5] M. LEBOUCHE, M. LUCIUS, Grandeurs caractéristiques en Rhéologie et Mécanique.Proceeding du 2nd congrès sur les Techniques Avancées en Hémorhéologie.Pp 75-131 NANCY (1983)
[6] Y. I. CHO, J. P. HARTNETT, Non-Newtonian fluids in circular pipe flow. Adv. Heat. Transfer, vol 15, Pp 67-69 (1982).
[7] W.L WILKINSON. Non Newtonian fluids. Pergamon Press (1960)
[8] ANSYS 14.0, Inc.
[9] Patankar, S. V., 1980, Numerical Heat Transfer and Fluid Flow, Hemisphere,Washington, D.C.
[10] Durst, F., Ray, S., Unsal, B., and Bayoumi, O. A., 2005, "The Development Lengths of Laminar Pipe and Channel Flows," ASME J. Fluids Eng., 127, pp. 1154–1160.
[11] L.L. Ferras, A.M. Afonso, M.A. Alves, J.M. Nobrega, F.T. Pinho, 2012, "Development Length in Planar Channel Flows of Newtonian Fluids Under the Influence of Wall Slip," ASME J. Fluid Eng.